Available online at www.sciencedirect.com

ScienceDirect

Current Opinion in Electrochemistry

Review Article

Review—Electrochemical impedance spectroscopy for lithium-ion batteries: Measurement and analysis (for automotive applications)

Rico Klink[1,2], René H. E. van Doorn[1] and André Weber[2]

Electrochemical impedance spectroscopy is a reliable tool for the electrochemical analysis of various types of electrochemical cells. It is commonly applied in research and development to deconvolute and quantify different electrochemical processes limiting the cell performance and to understand ageing phenomena in the cell. Due to its performance, electrochemical impedance spectroscopy is increasingly considered to be used on the system level in commercial applications of electrochemical cells.
In this contribution, recent approaches to apply electrochemical impedance spectroscopy in automotive lithium-ion battery systems are reviewed. We will discuss advanced measurement, data analysis and modelling approaches that provide access to essential information of the battery's state and show a potential to meet the requirements of automotive battery systems.

Addresses
[1] AUDI AG, NSU-Str. 1, 74172 Neckarsulm, Germany
[2] Institute for Applied Materials – Electrochemical Technologies (IAM-ET), Karlsruhe Institute of Technology (KIT), 76131 Karlsruhe, Germany

Corresponding author: Klink, Rico (rico.klink@audi.de), (rico.klink@kit.edu)

Current Opinion in Electrochemistry 2025, **54**:101768

This review comes from a themed issue on **Electrochemical Impedance Spectroscopy (EIS) (2025)**

Edited by **Mark E. Orazem** and **Vincent Vivier**

For complete overview about the section, refer Electrochemical Impedance Spectroscopy (EIS) (2025)

Available online 10 October 2025

https://doi.org/10.1016/j.coelec.2025.101768

Introduction

In the last decades, **electrochemical impedance spectroscopy** (EIS) has become a well-established tool for lithium-ion battery cell analysis. Fundamentals of EIS are described in a number of handbooks [1–4]. Since the work of Aurbach [5], EIS has been widely applied for Li-ion battery research and development, its actuality is exemplarily shown by Nunes [6,7] and Teki [8].

Conventional EIS, due to its consecutive single frequency measurement methodology, is not expedient for automotive applications. Its boundary conditions regarding linearity, time invariance and causality are hardly fulfilled during car operation. The high-capacity, low-resistance cells used in propulsion applications lead to challenges regarding EIS hardware and bit resolution during (*in situ*) analysis and modelling [9,10].

Nevertheless, EIS is considered for monitoring automotive relevant parameters like **S**tate **o**f **C**harge (SOC), **S**tate **o**f **H**ealth (SOH) and cell temperature in battery systems [11]. In this review, recent developments in advanced excitation methods and data analysis approaches for automotive use cases are discussed.

Excitation signals

Apart from standard consecutive frequency EIS, different impedance measurement strategies are being discussed in the literature. Figure 1 provides an overview on the excitation and subsequent signal processing routes. A distinction must be made between sinusoidal and binary excitations. Standard sinusoidal current or voltage stimuli as well as the typical step signal are directly useable for interpretation. Even with single-sine excitation, impedance values are typically calculated using discrete Fourier transformation. For all other signal excitations, a time-to-frequency domain transformation is necessary, requiring additional computing costs to be considered for *in situ* car measurements.

Based on the overview in Figure 1, Figure 2 shows examples for signal excitation and resulting.

Standard EIS

Traditionally, the impedance is measured at consecutive discrete frequencies by a sinusoidal current or voltage stimulus correlated with the resulting voltage or current response (Figure 2A1) and phase shift in signal. This approach concentrates the excitation on the frequency of interest and, as long as linearity requirements are fulfilled, avoids any higher harmonics. At the expense of time and costly equipment, it enables a high impedance data quality. While the methodology offers clear benefits, these must be critically evaluated in light of potential disadvantages, including time consumption, financial

Figure 1

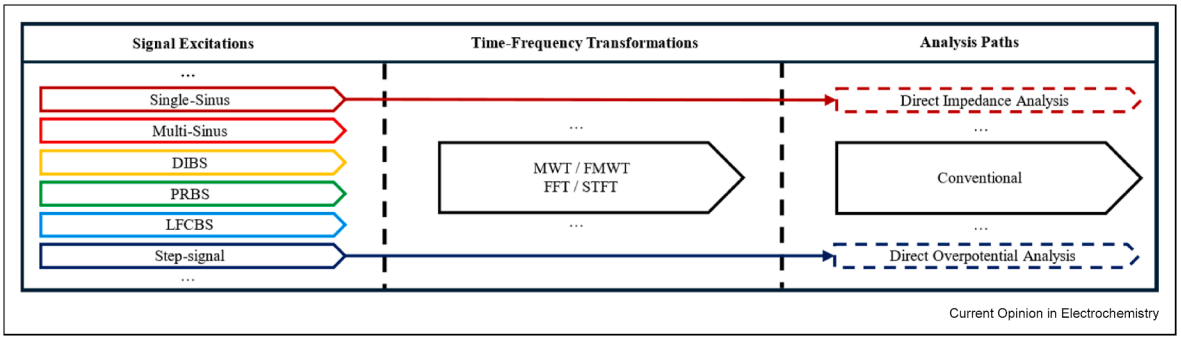

Different signal excitations and its various analysis paths.

Figure 2

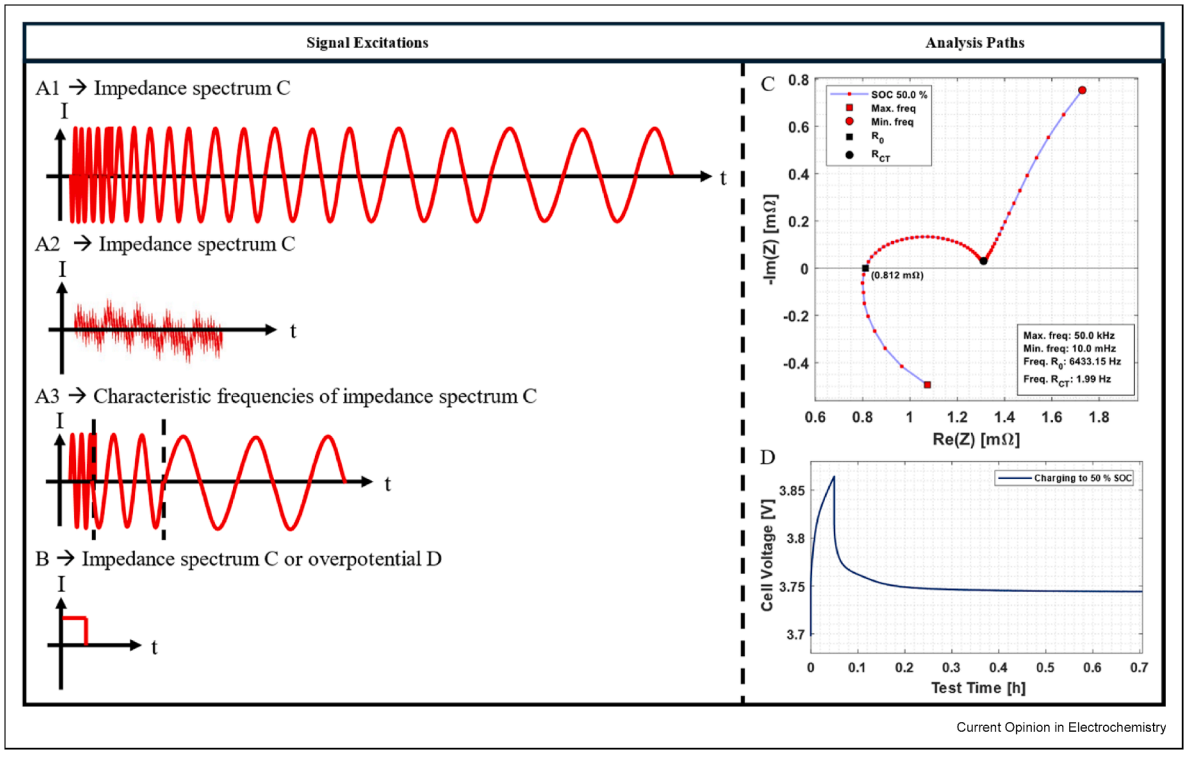

Different EIS techniques. Left signal, right processed data. **A1:** standard EIS, **A2:** multi-sinus both with response **C**, **A3:** characteristic frequency measurement with characteristic frequency impedance in **C** (black markers), **B**: Step/binary excitation, with response **C** after FFT or **D** in time domain, data after [12]. EIS, electrochemical impedance spectroscopy; FFT, fast Fourier transformation.

cost, and the necessity for vehicle standstill during and before measurement. To reduce these disadvantages, several alternative approaches are being developed.

Multisine EIS

The idealised multisine approach enables a shortening of the measurement duration, without loss of datapoints. This is realised by stimulation with multiple overlapping sinusoidal stimuli (Figure 2A2). Based on a specific number of frequency points, a wide impedance spectrum can be calculated (Figure 2C). Challenges regarding phase optimisation, power levelling of the single frequencies as well as frequency selection have to be considered, ensuring a high measurement quality [13–16].

For automotive cells with a specific capacity exceeding 100 Ah, the most relevant frequency range typically lies below 100 Hz. In particular, the charge transfer resistance is often most pronounced at frequencies below 1.5 Hz. A known limitation of multisine EIS is its reduced frequency resolution at low frequencies (impacting diffusion frequency analysis), due to the requirement that excited frequencies be integer multiples of a fundamental frequency—resulting in imperfect logarithmic spacing and potential information loss. In particular, high memory capacity is required in potentiostats to handle wideband multisine signals and large volumes of data. Hence, this comes at the expense of computational power and costly equipment. In comparison, this approach allows measurements to be taken during vehicle operation not only during parking. In the context of automotive applications, where cost-effectiveness is essential, a critical evaluation of the benefits and limitations of this methodology is required.

Characteristic frequency measurement

Provided that the characteristic frequencies of the system are known, and remain constant across different system states (temperature, SOC and SOH), one can measure at characteristic points only (Figure 2A3). Lazanas and Prodromidis [17] point out the correspondence of single frequencies to the ohmic resistance and to the maximum imaginary parts of the impedance. According to Chang et al. [18], a calculation of impedance at low frequencies based on a few measurement points at mid- or high frequencies is possible (as illustrated by single measurement points in Figure 2C). In general, nested impedance features can be used for fast state calculations. A well-known example of this approach is the measurement of the internal battery resistance at $f = 1$ kHz. Details of this approach are described in Specific Car Issues – SOH estimation. The assumption of constant characteristic frequencies for measuring individual impedance properties carries a very high risk of error. This simplification is only valid if there is sufficient knowledge about the properties of the specific cell system and its ageing behaviour.

Binary signals

Alternatively, other signal forms can be used for stimulation, such as pulse or step functions in current or potential, respectively, as shown in Figure 2B. For batteries, the subsequent time-dependent response of the (over)potential after the pulse is commonly analysed (Figure 2D).

A distinction between single-step signal excitation and recurring signals like **d**iscrete-**i**nterval **b**inary **s**equences (DIBSs) [19,20] and **p**seudo**r**andom **b**inary **s**equences (PRBSs) [20,21] have to be made. DIBS transforms multisine excitation into discrete binary sequences employing equation (2.1) [19]:

$$b(t) = \operatorname{sign}\left(\sum_{n=1}^{N} a_n \sin\left(2\pi f_n t + \phi_n\right)\right) \qquad 2.1$$

PRBS uses pseudo random sequences like the maximum length sequence, which can be generated by using a linear-feedback shift register [21].

All wideband signals, whether binary or multisine, have the problem of wide-spread energy. The excitation energy used for single frequencies is quite low. As a result, the signal-to-noise ratio (SNR) can be insufficient. Focussing on low-frequency behaviour, Geng et al. [20] implemented a **l**ow-**f**requency **c**oncentrated **b**inary **s**ignal. Additionally, the useable frequency range is constrained by the steepness of the pulse edges of the excitation signal and the sampling frequency. With sinusoidal signal excitation forms (e.g. standard EIS), this limitation does not exist. The advantage of significantly more affordable hardware compared to multisine excitation comes at the cost of a lower SNR in the high-frequency range. However, the dominant frequency spectrum of large-format automotive cells lies in the low-frequency range, which helps to limit the associated costs.

Analysis of the response curve can either be performed directly in the time domain (Figure 2E) or after transformation into the frequency domain (Figure 2C). The transformation of the time-based signals into frequency domain can generally be done in different ways: standard transformation methods are the **F**ast **F**ourier **T**ransformation (**FFT**) as well as the **M**orlet **W**avelet **T**ransformation (MWT) with its application-specific simplifications, **S**hort **T**ime **F**ourier **T**ransformation and **F**ast-**MWT** [20] (Figure 1).

The cost-benefit assessment of the discussed technologies must be carried out individually for each vehicle segment and its intended operating conditions. One of the initial challenges lies in the changing boundary conditions during vehicle use. Depending on the operating state—driving, charging, or parking—certain measurement principles may be more or less suitable.

Specific car issues

Propulsion battery systems

Compared to standard (consumer) batteries, propulsion batteries present specific challenges. Having cell capacities well above 100 Ah, (pseudo) internal resistance needs to be in the low single digit mΩ range. Additional limitations regarding current load capacity have to be considered. Small internal ohmic resistances of $R_0 < 1.0$ mΩ are common (Figure 2). This requires current stimuli exceeding 10 A to generate a voltage excitation in the range of 10 mV. The useable minimum signal perturbation depends on the SNR.

To reach a traction relevant voltage level, 100−200 cells are connected in series, frequently several of which are in parallel as well, easily resulting in 400+ cells to be individually monitored. The typical solution being the use of several **C**ell **M**odule **C**ontrollers (CMCs), each of which measures the single cell potential of a number of cells as well as a selected number of temperatures, being broadcasted through a battery internal network to a central **B**attery **M**anagement **C**ontroller (BMC) which is the gateway to the rest of the car.

Battery system measurement

The aforementioned issues result in specific measurement challenges. The extremely low impedance severely hampers standard nonlinear least square−based parameter determination as the values are on the order of the standard squared error, hence processor byte level resolution [22]. Furthermore, due to the serial character of the battery system, each single cell has to be analysed. Monitoring the entire pack would not allow detection of cell-specific failures. For cost reasons, the single cells could be measured employing a MOSFET multiplexer as shown by Zhang et al. [23]. An alternative approach by Blömeke et al. [24] implements balancing resistor-based EIS by using the existing balancing hardware. Based on [24], the main problems are the voltage measurement as well as the high heat generation due to resistance based power dissipation.

Due to cost and size restrictions, automotive EIS/BMC setups try to use single-chip designs. Datang NXP introduced the BMC chip DNB1101A with integrated EIS measurement in the year 2022 [25]. With the focus on automotive applications, Marelli announced a BMC with standard sweeping EIS measurement at the CTI Symposium Berlin 2024 [26]. Both chips are working with single-sinus excitations. Providing high measurement data resolutions and measurement speed, EIS-suitable BMC systems ('EIS-ready') are marketed. Examples are from Infineon with its TLE9018DQK [27] or from Texas Instruments with its BQ79616-Q1 series [28]. Analog Devices exemplarily developed the AD5940/AD5941 series, a front end with EIS measurement functionality [29]. The described systems for EIS measurement are primarily intended for measurements in a steady-state condition. Operando EIS or real-time dynamic EIS methods use optimised multisine signals or special binary sequences (such as DIBS) to significantly reduce measurement time [30,31]. Research also focuses on superimposing charging or operating currents with small current excitations or utilising natural current changes [32]. Considering the challenges described in the subsection 'Propulsion battery systems', wide-spread application is still pending, although patent submissions already exist.

Zhang et al. [23] developed a method based on an equivalent sampling, ignoring the Nyquist sampling limits law. Their calculation model achieved robustness in frequencies from a few Hz to kHz. Validation of the measurements based on the diagnostic of lithium plating, focussing on the shape and size of the semicircles, yielded reliable results with errors up to 0.6 mΩ (<0.8 %).

To fulfil the requirement of time invariance, measurements should only be performed in the resting state after compensatory processes have subsided, which implies an active high voltage system at standstill. In this context, standstill as well as parking refer to a current of $I = 0$. Depending on the system's history (duration, direction and amplitude of current load, temperature, SOC, and SOH), different waiting periods (relaxation times) are required before the system can be considered as time-invariant ($\Delta V/t <$ threshold). These relaxation times range from a few hours to several days. Particularly, full cells based on primary lithium iron phosphate (LFP) chemistry, with a high degree of electrode utilisation on both sides, exhibit disproportionately long relaxation times exceeding 100 h, especially at low states of charge. On top of this, ageing effects are typically observable in the μHz range, violating linearity requirements and need hours per frequency.

High excitation signals, low-frequency measurements and the superposition with DC current, all lead to a nonlinear cell behaviour. A possible way to detect this is the use of Lissajous plots in the case of single sinus EIS [33]. Alternatively, the direct detection out of the signal spectrum is possible. Nonlinearity results in the presence of higher order harmonics [33]. Nonstationarity can typically be detected effectively at low frequencies due to the presence of drift spectra and so-called "skirts"—spectral components surrounding the excited frequencies.

Ji and Schwartz [34,35] employed the second harmonic of nonlinear EIS to develop a more comprehensive model of full-cell behaviour than is achievable with conventional EIS. The modelling effort is high and requires half-cell measurements for a parameter input. An alternative approach for model parametrisation based on the second harmonic was developed by Kirk et al. [36]. A more applied use case was investigated by Ulrich et al. [37], using the nonlinear frequency response analysis for detection of lithium plating. The approach shows potential for automotive applications aiming at lithium plating detection during fast charging (alternating between fast charging and nonlinear EIS). The use of precise equipment, as well as the switch between charging current and sinusoidal excitation, remains challenging but offers promising potential for future applications.

It is well known that different electrode processes exhibit temperature, SOC- and SOH-dependent

behaviour. Hence, EIS-based analysis of these parameters is suitable for single-cell diagnostics. When focussing on multicell systems, which by nature exhibit nonuniform behaviour among individual cells, this results in significantly different state characteristics.

In the following subsections, current approaches to the estimation of these states are presented.

Internal cell temperature measurement

Typically, the temperature inside the cell of a traction battery is determined by temperature sensors in the battery module combined with thermal battery models. Although a simple straightforward approach, the relevant core temperature of the cell can, at best, be estimated. EIS can be employed for monitoring the internal cell temperature due to its extreme sensitivity to temperature changes [38,39]. Older approaches correlate a characteristic single-frequency measurement (mainly at the intercept frequency) with the core temperature of the cell [38]. Yet problems regarding different sensitivity of the impedance at different temperatures and frequencies as well as a decoupling from SOC, SOH and nonlinear *in situ* car measurements exist. Shen et al. [40] proposed a new methodology by using a temperature calculation algorithm based on a two-step estimation to circumvent these issues. In a first step, the cell core temperature is calculated based on the ambient and surface temperature of the cell. In a subsequent step, the ideal frequency for EIS measurement, based on this estimate, is selected. In an iterative process, based on EIS measurement, a new core temperature is calculated. This new core temperature is used to calculate a new, better frequency for EIS measurements and optimise temperature calculation once more. An additional approach from Li et al. [41] focuses on the multifrequency imaginary part impedance in combination with a machine learning algorithm. In the first step, they characterised the impedance based on temperature, SOC, and SOH. With the Pearson correlation, they separated imaginary part points which correlate to temperature. In a second step, employing Gaussian process regression, the core temperature is calculated. A disadvantage is that a sufficiently large data set is required in order to accurately estimate the cell's core temperature.

Considering the necessary equipment and efforts to determine the cell temperature via EIS, it can be stated that the application of EIS for temperature measurements only is not meaningful. However, if EIS is applied for a more detailed battery analysis as described in the following chapters, the additional information about the temperature of the different cells will become available and can be applied in an enhanced thermal control strategy for the battery system.

SOC estimation

In [42], Demirci et al. reviewed different SOC estimation methods. Due to the high experimental requirements, they concluded that EIS is not a practical approach.

Despite these considerations, a trend towards "indirect" usage of EIS data is currently observable. In this case, EIS is used to obtain specific parameters in a laboratory surrounding, which are then used for different concepts to determine the SOC in the car. Such an approach dealing with the estimation of fractional SOC based on open circuit voltage (OCV) hysteretic characteristics was published by Chen et al. [43] They combined the SOC−OCV estimation model with a fractional second-order ohmic resistance in parallel with a constant phase element equivalent circuit model (ohmic resistance in parallel with a constant phase element). A correction of the SOC estimation based on charging/discharging history and relaxation times improves the SOC calculation although ageing-dependent changes of OCV characteristics are not considered. A problem arises when calculating the SOC of typical LFP cells. Che et al. [44] assessed a combination of coulomb counting, machine learning and relaxation behaviour for SOC estimation in LFP systems. Their approach shows a relatively high error in the SOC estimate. Lu et al. [45] proposed reducing the SOC calculation effort by using linearisation of voltage hysteresis curves and a linear neural network using voltage signal data, its deviation, and the historical current direction to calculate SOC.

Despite the complexity of using EIS for SOC estimation, the combination of determining (parts of) an EIS spectrum that is analysed by machine learning algorithms is under development. Kong et al. [46] used frequency-dependent features of EIS caused by diffusion characteristic for SOC calculation. Buchicchio et al. [47,48] combined data-driven machine learning with equivalent circuit models. It is pointed out that the usage of circuit parameters instead of direct impedance values from EIS improves the accuracy and efficiency of calculation. The usage of machine learning algorithms like 2D convolutional neural networks seems to be target-aimed. Additional approaches focussing on the EIS-based SOC estimation for aged batteries are from Wang et al. [49] as well as from Anekal and Williamson [50].

The latter approaches are meaningful as the impedance spectra of the considered cells are monitored and, next to information about the SOH discussed in the next section, provide a higher accuracy in SOC calculation. It should be noted that accurate and up-to-date values of the battery's internal resistance are not only supporting SOC determination but also driving range predictions.

SOH estimation

SOH estimation by means of EIS is by far the most complex topic as various ageing mechanisms can simultaneously affect different frequency ranges in the impedance spectrum. A direct SOH calculation method was proposed by Pang et al. [51], based on a two-frequency measurement (frequency 1: the gain cross-over frequency, frequency 2: the charge transfer resistance corner frequency). The SOH shift is given by equation (3.1).

$$n_{SOH} = \frac{Z_{real\ freq.\ 1}}{Z_{real\ freq.\ 2}} \tag{3.1}$$

Xing et al. [52] described an approach interpreting EIS data based on transferring information from reference cells to predict SOH. It assumes a good knowledge of cell-specific ageing. However, it employs a state of the battery hardly present in cars and is difficult to apply in a continuously changing cell development process. Another approach by Li et al. [53] combines a data-driven methodology with EIS-based equivalent circuit models to evaluate SOH. They pointed out different categories of data-driven methods for using the impedance data on SOH calculation. Complete EIS data at different temperatures and SOH levels are used, in combination with an autoencoder-based neural network, for SOH calculation [54].

Employing their minimalistic measurement approach, Chang et al. [18] used only a few data points from the medium–high frequency segments measured via EIS. With a sparrow search algorithm optimised network, it is possible to extrapolate the impedance at the low-frequency segments. However, this calculation method has to be used carefully. Mombrini et al. [55], for instance, studied the change of the phase transition in active materials over the lifetime. The coexistence of different lithiation stages results in a changing phase transition and as a consequence in changing diffusion characteristics, which affect the impedance behaviour in low-frequency segments. In light of changes in phase transition over cell lifetime, a direct correlation between charge transfer in the mid-frequency range and diffusion behaviour in the low-frequency range is not guaranteed.

Employing a neural network, Gao et al. [56] used six characteristic feature points of the Nyquist plot and their change over lifetime for calculating SOH. Employing small relatively high ohmic coin cells, their methodology showed promising results, although further analysis including SOC and temperature dependencies for the EIS measurements have to be performed.

Considering that the SOH of an automotive battery is accessible via the charging/discharging capacity and the battery performance in different states, a general SOH determination via EIS is not mandatory but can be a useful tool to track ageing processes and detect critical states of the cells in an early stage.

Summary and outlook

EIS for lithium-ion batteries is reviewed, focussing on recent progress in measurements and analysis for automotive applications, along with a description of typical high-capacity cell specifics. Measurement techniques based on sinusoidal excitation are distinguished from those using binary signals.

Despite recent improvements in cost and time as well as the significantly grown experience and knowledge on EIS, direct *in situ* application of EIS in vehicles remains difficult due to low internal resistances, cell switching requirements, and hardware limitations. Practical solutions are still in the research state. The application of EIS under operating conditions (charging, driving, and parking) requires expensive hardware as well as sufficiently advanced data processing capabilities. The benefits of enhanced state estimation are currently outweighed by the high costs associated with vehicle integration. Applying EIS remains technically demanding and economically challenging.

Applications under investigation are temperature, SOC, and SOH estimation. Temperature determination remains typically sensor-based and is supported by thermal modelling. For SOC estimation, indirect methods based on time-resolved overpotential measurements are prevalent, alongside machine learning approaches. LFP cells pose a specific challenge due to their voltage and current characteristics as well as their phase change behaviour. To improve SOC accuracy as well as SOH estimation using EIS, new approaches primarily relying on neural networks and data-driven models are proposed in the literature.

The highest potential for practical application is seen in the combination of artificial intelligence-based modelling with EIS. This is a rapidly evolving field, and further applications are expected in the near future.

CRediT author statement

Rico Klink: Conceptualization, Visualization, Writing – Original draft. **René H. E. van Doorn:** Supervision, Writing – review & editing. **André Weber:** Supervision, Writing – review & editing.

Declaration of competing interest

The authors declare that they have no known competing financial interests or personal relationships that could

have appeared to influence the work reported in this paper.

Acknowledgements
The authors would like to thank the employees of AUDI AG and KIT for the constructive discussions during the preparation of this paper.

Data availability
No data was used for the research described in the article.

References
Papers of particular interest, published within the period of review, have been highlighted as:

* of special interest
** of outstanding interest

1. Macdonald JR: **Impedance spectroscopy**. *Ann Biomed Eng* 1992, **20**:289–305, https://doi.org/10.1007/BF02368532.

2. Macdonald JR: **Impedance spectroscopy: old problems and new developments**. *Electrochim Acta* 1990, **35**:1483–1492, https://doi.org/10.1016/0013-4686(90)80002-6.

3. Barsoukov E, Macdonald JR: *Impedance spectroscopy: theory, experiment, and applications*. 2 ed. Hoboken NJ: Wiley-Interscience; 2005. ISBN:°0-471-64749-7.

4. Orazem ME, Tribollet B: *Electrochemical impedance spectroscopy. The electrochemical society series*. Hoboken, NJ: John Wiley & Sons, Inc.; 2008. ISBN: 978-0-470-04140-6.

5. Aurbach D, Levi MD, Levi E, Teller H, Markovsky B, Salitra G, *et al*.: **Common electroanalytical behavior of Li intercalation processes into graphite and transition metal oxides**. *J Electrochem Soc* 1998, **145**:3024–3034, https://doi.org/10.1149/1.1838758.

6. Nunes H, Martinho J, Fermeiro J, Pombo J, Mariano S, Calado MdR: **Impedance analysis and parameter estimation of lithium-ion batteries using the EIS technique**. *IEEE Trans Ind Appl* 2024, **60**:5048–5060, https://doi.org/10.1109/TIA.2024.3365451.

7. Nunes H, Martinho J, Fermeiro J, Pombo J, Mariano S, Calado MDR: **Impedance analysis of a lithium-ion battery using the electrochemical impedance spectroscopy**. In *2022 IEEE international conference on environment and electrical engineering and 2022 IEEE industrial and commercial power systems Europe (EEEIC/I&CPS Europe)*; 2022:1–7, https://doi.org/10.1109/EEEIC/ICPSEurope54979.2022.9854629.

8. Teki VK, Kasi J, Chidurala S, Priyadarshini S, Joga SRK, Maharana MK, *et al*.: **Analysis of lithium-ion batteries through electrochemical impedance spectroscopy modeling**. *J Electrochem Soc* 2024, **171**, 060528, https://doi.org/10.1149/1945-7111/ad561f.

9. Ria A, Manfredini G, Gagliardi F, Vitelli M, Bruschi P, Piotto M: **Online high-resolution EIS of lithium-ion batteries by means of compact and low power ASIC**. *Batteries* 2023, **9**:239, https://doi.org/10.3390/batteries9050239.

10. Fabozzi M, Ramilli R, Crescentini M, Traverso PA: **A low-cost electrochemical impedance spectroscopy-based sensor node for online battery cell monitoring**. In *2024 IEEE international workshop on metrology for automotive (MetroAutomotive)*; 2024:112–117, https://doi.org/10.1109/MetroAutomotive61329.2024.10615588.

11. Menye JS, Camara M-B, Dakyo B: **Lithium battery degradation and failure mechanisms: a state-of-the-art review**. *Energies* 2025, **18**:342–384, https://doi.org/10.3390/en18020342.

12. Klink R, Schiffler M, Weber A: *To be published - impedance and overpotential characteristic of lithium-ion batteries*. 2026.

13. Zheng X, Bai J: **Wideband impedance detection method for energy storage batteries**. In *2023 5th international academic exchange conference on science and technology innovation (IAECST)*; 2023:1699–1702, https://doi.org/10.1109/iaecst60924.2023.10502516.

14. Liu Z, Wang X, Chang G, Yuan H, Tang W, Wei X, *et al*.: **Online monitoring of fuel cell electrochemical impedance spectrum with multi-stages multi-sine signals based on DC–DC converter**. *IEEE Trans Power Electron* 2024, **39**:16826–16838, https://doi.org/10.1109/tpel.2024.3448530.

15. Al-Ali A, Elwakil AS, Maundy B, Majzoub S, Allagui A: **Electrical impedance spectroscopy using a wide-band signal based on the rudin-shapiro polynomials**. *J Electrochem Soc* 2023, **170**, 047501, https://doi.org/10.1149/1945-7111/acc7cf.

16. Akparibo A, Barendse P: **A hybrid perturbation technique for wideband online impedance spectroscopy measurements of PV panels using a DC-DC converter**. In *2024 IEEE energy conversion congress and exposition (ECCE)*; 2024:407–413, https://doi.org/10.1109/ecce55643.2024.10861005.

17. Lazanas AC, Prodromidis MI: **Electrochemical impedance Spectroscopy-A tutorial**. *ACS Meas Sci Au* 2023, **3**:162–193, https://doi.org/10.1021/acsmeasuresciau.2c00070.

18. * Chang C, Pan Y, Wang S, Jiang J, Tian A, Gao Y, *et al*.: **Fast EIS acquisition method based on SSA-DNN prediction model**. *Energy* 2024, **288**, 129768, https://doi.org/10.1016/j.energy.2023.129768.
This work uses a deep learning-based method for predicting impedance spectra based on fragmented data significantly reducing measurement time. Using a sparrow search algorithm optimised network, high frequency impedance measurement points are employed to reconstruct low-frequency impedance data.

19. Liu X, Tao S, Fu S, Ma R, Cao T, Fan H, *et al*.: **Binary multi-frequency signal for accurate and rapid electrochemical impedance spectroscopy acquisition in lithium-ion batteries**. *Appl Energy* 2024, **364**, 123221, https://doi.org/10.1016/j.apenergy.2024.123221.

20. Geng A, Hu H, Peng Y, Zhao Z, He Z, Gao S: **Wideband measurement approach for EIS of lithium-ion batteries using low-frequency concentrated disturbance**. *IEEE Trans Ind Electron* 2024, **71**:4851–4860, https://doi.org/10.1109/tie.2023.3286005.

21. Du X, Meng J, Peng J: **Hybrid pseudorandom sequence for broadband impedance measurements of lithium-ion batteries**. *IEEE Trans Ind Electron* 2023, **70**:6856–6864, https://doi.org/10.1109/TIE.2022.3201347.

22. Boukamp BA: **A nonlinear least squares fit procedure for analysis of immittance data of electrochemical systems**. *Solid State Ionics* 1986, **20**:31–44, https://doi.org/10.1016/0167-2738(86)90031-7.

23. Zhang S, Wei Z, Zhang L, Hu J, Dai R: **Equivalent sampling-enabled module-level battery impedance measurement for in-situ lithium plating diagnostic**. *J Power Sources* 2024, **600**, 234239, https://doi.org/10.1016/j.jpowsour.2024.234239.

24. Blömeke A, Zappen H, Ringbeck F, Frie F, Wasylowski D, Sauer DU: **Balancing resistor-based online electrochemical impedance spectroscopy in battery systems: opportunities and limitations**. *Commun Eng* 2024, **3**:1–9, https://doi.org/10.1038/s44172-024-00203-6.

25. Semiconductors DN: *Datang NXP: the successful commercialization of EIS technology is expected to usher in changes in the new energy industry*. 2022 [cited 15.06.2025]; Available from: https://www.datangnxp.com/en/details/news/63.

26. Marelli: *Marelli unveils latest innovative battery management systems solution at CTI symposium Berlin 2024*. 2024 [cited 15.06.2025]; Available from: https://www.marelli.com/en/news/marelli-unveils-latest-innovative-battery-management-systems-sol.html.

27. infineon: *TLE9018DQK - Li-Ion battery monitoring and balancing IC*. 2025 [cited 15.06.2025]; Available from: https://www.infineon.com/cms/de/product/battery-management-ics/tle9018dqk/.

28. Texas_Instruments: *BQ79616-Q1 16-S automotive precision battery monitor, balancer and integrated protector with ASIL-D*

compliance. 2021 [cited 16.06.2025]; Available from: https://www.ti.com/product/BQ79616-Q1.

29. ANALOG_DEVICES: ***AD5941 high precision, impedance & electrochemical front end*** [cited 15.06.2025]; Available from: https://www.analog.com/en/products/ad5941.html.

30. Hao Z, Wang X, Wei X, Dai H: **Fast and highly accurate measurement of electrochemical impedance spectra of power batteries based on optimized multi-sine signals**. *Measurement* 2025, **252**, 117355, https://doi.org/10.1016/j.measurement.2025.117355.

31. Tran M, Roinila T, Markkula J: **Realtime internal-impedance measurement of lithium-ion battery using discrete-interval-binary-sequence injection**. In *2022 IEEE energy conversion congress and exposition (ECCE)*; 2022, https://doi.org/10.1109/ECCE50734.2022.9947434.

32. Sihvo J, Stroe DI: **Real-time impedance monitoring of Li-ion batteries under dynamic operating conditions using the discrete fourier transform eigenvector approach**. *Cell Rep Phys Sci* 2025, **6**, 102512, https://doi.org/10.1016/j.xcrp.2025.102512.

33. Zabara MA, Goh JM, Gaudio VM, Zou L, Orazem ME, Ulgut B: **Utility of lissajous plots for electrochemical impedance spectroscopy measurements: detection of NonLinearity and non-stationarity**. *J Electrochem Soc* 2024, **171**, 010507, https://doi.org/10.1149/1945-7111/ad19eb.

34. Ji Y, Schwartz DT: **Second-harmonic nonlinear electrochemical impedance spectroscopy: part I. Analytical theory and equivalent circuit representations for planar and porous electrodes**. *J Electrochem Soc* 2023, **170**, 123511, https://doi.org/10.1149/1945-7111/ad15ca.

35. Ji Y, Schwartz DT: **Second-harmonic nonlinear electrochemical impedance spectroscopy: part II. model-based analysis of lithium-ion battery experiments**. *J Electrochem Soc* 2024, **171**, 023504, https://doi.org/10.1149/1945-7111/ad2596.

36. Kirk TL, Lewis-Douglas A, Howey D, Please CP, Jon Chapman S: **Nonlinear electrochemical impedance spectroscopy for lithium-ion battery model parameterization**. *J Electrochem Soc* 2023, **170**, 010514, https://doi.org/10.1149/1945-7111/acada7.

37. ** Ulrich J, Lindner A, Brake T, Winter M, Wiemers-Meyer S, Weber A, *et al*.: **Early detection of lithium plating during fast charging of lithium-ion batteries using nonlinear frequency response analysis**. *J Power Sources* 2025, **647**, 237358, https://doi.org/10.1016/j.jpowsour.2025.237358.
This study reveals that nonlinear frequency response analysis, particularly the second harmonic of impedance measurement response, offers a sensitive method for the early detection of lithium plating during battery charging. A developed cell model simulates plating, enabling operando diagnostics and providing deeper insight into intercalation kinetics.

38. Pan Y, Xu K, Chen Z, Wang K: **Advanced techniques for internal temperature monitoring in lithium-ion batteries: a review of recent developments**. *Coatings* 2025, **15**:268, https://doi.org/10.3390/coatings15030268.

39. Schmidt JP, Arnold S, Loges A, Werner D, Wetzel T, Ivers-Tiffée E: **Measurement of the internal cell temperature via impedance: evaluation and application of a new method**. *J Power Sources* 2013, **243**:110–117, https://doi.org/10.1016/j.jpowsour.2013.06.013.

40. * Shen Z, Dai F, Jiao F, He Y: **Predicting the internal temperature of lithium batteries based on frequency impedance spectroscopy**. *Proceedings of the CSEE* 2025, **45**:1913–1921, https://doi.org/10.13334/j.0258-8013.pcsee.232237.
This study proposes a multi-frequency EIS-based method for estimating internal battery temperature, achieving high accuracy under varying discharge currents and outperforming single-frequency approaches. An iterative two-step process is used to identify the optimal decoupled EIS measurement frequency for estimating the cell core temperature.

41. Li J, Li T, Qiao Y, Tan Z, Qiu X, Deng H, *et al*.: **Internal temperature estimation method for lithium-ion battery based on multi-frequency imaginary part impedance and GPR model**. *J Energy Storage* 2025, **118**, 116287, https://doi.org/10.1016/j.est.2025.116287.

42. Demirci O, Taskin S, Schaltz E, Acar Demirci B: **Review of battery state estimation methods for electric vehicles - part I: SOC estimation**. *J Energy Storage* 2024, **87**, 111435, https://doi.org/10.1016/j.est.2024.111435.

43. Chen H, Liu F, Hou H, Shen X: **Estimation of fractional SOC for lithium batteries based on OCV hysteretic characteristics**. *Ionics* 2024, **30**:2627–2641, https://doi.org/10.1007/s11581-024-05442-3.

44. Che Y, Xu L, Teodorescu R, Hu X, Onori S: **Enhanced SOC estimation for LFP batteries: a synergistic approach using coulomb counting reset, machine learning, and relaxation**. *ACS Energy Lett* 2025, **10**:741–749, https://doi.org/10.1021/acsenergylett.4c03223.

45. Lu C, Hu J, Zhai Y, Hu H, Zheng H: **State of charge estimation method based on linearization of voltage hysteresis curve**. *J Energy Storage* 2023, **72**, 108481, https://doi.org/10.1016/j.est.2023.108481.

46. Kong L, Fang S, Niu T, Chen G, Liao R: **Fast state of charge estimation for lithium-ion battery based on electrochemical impedance spectroscopy frequency feature extraction**. In *2023 IEEE/IAS 59th industrial and commercial power systems technical conference (I&CPS)*; 2023:1–8, https://doi.org/10.1109/icps57144.2023.10142117.

47. * Buchicchio E, De Angelis A, Santoni F, Carbone P, Bianconi F, Smeraldi F: **Battery SOC estimation from EIS data based on machine learning and equivalent circuit model**. *Energy* 2023, **283**, 128461, https://doi.org/10.1016/j.energy.2023.128461.
This paper presents the correlation between the SOC and EIS measurements, along with an additional SOC estimation approach based on EIS data using machine learning and equivalent circuit modelling (ECM). The proposed method successfully validates the frequency- and time-domain behaviour across different cells.

48. * Buchicchio E, De Angelis A, Santoni F, Carbone P: **Uncertainty characterization of a CNN method for lithium-ion batteries state of charge estimation using EIS data**. *Measurement* 2023, **220**, 113341, https://doi.org/10.1016/j.measurement.2023.113341.
Bucchiccio et al. presented a machine learning approach for SOC estimation using EIS data and a two-dimensional convolutional neural network. By using circuit parameters instead of raw impedance data, the approach improves accuracy and efficiency.

49. Wang L, Zhao X, Deng Z, Yang L: **Application of electrochemical impedance spectroscopy in battery management system: state of charge estimation for aging batteries**. *J Energy Storage* 2023, **57**, 106275, https://doi.org/10.1016/j.est.2022.106275.

50. Anekal L, Williamson S: **Adaptive battery state-of-charge estimation using aging-driven equivalent circuit parameterization and electrochemical impedance spectroscopy**. In *2024 IEEE transportation electrification conference and expo (ITEC)*; 2024:1–6, https://doi.org/10.1109/itec60657.2024.10599079.

51. Pang Z, Yang K, Song Z, Niu P, Chen G, Meng J: **A new method for determining SOH of lithium batteries using the real-part ratio of EIS specific frequency impedance**. *J Energy Storage* 2023, **72**, 108693, https://doi.org/10.1016/j.est.2023.108693.

52. Xing Q, Zhang M, Fu Y, Wang K: **Transfer learning to estimate lithium-ion battery state of health with electrochemical impedance spectroscopy**. *J Energy Storage* 2025, **110**, 115345, https://doi.org/10.1016/j.est.2025.115345.

53. Li C, Yang L, Li Q, Zhang Q, Zhou Z, Meng Y, *et al*.: **SOH estimation method for lithium-ion batteries based on an improved equivalent circuit model via electrochemical impedance spectroscopy**. *J Energy Storage* 2024, **86**, 111167, https://doi.org/10.1016/j.est.2024.111167.

54. Obregon J, Han Y-R, Ho CW, Mouraliraman D, Lee CW, Jung J-Y: **Convolutional autoencoder-based SOH estimation of**

lithium-ion batteries using electrochemical impedance spectroscopy. *J Energy Storage* 2023, **60**, 106680, https://doi.org/10.1016/j.est.2023.106680.

55. Mombrini I, Heenan TMM, Checchia S, Jnawali A, Tan C, Johnson MJ, *et al*.: **Operando phase transition mapping of the negative electrode of a Li-ion 18 650 battery at high C-rates through fast synchrotron XRD-CT measurements**. *Sustain Energy Fuels* 2025, **9**:1848–1858, https://doi.org/10.1039/d4se00358f.

56. Gao Z, Jin Y, Zhang Y, Zhang Z, Li S, Liu J, *et al*.: **Static EIS multi-frequency feature points combined with WOA-BP neural network for Li-ion battery SOH estimation**. *Measurement* 2025, **253**, 117780, https://doi.org/10.1016/j.measurement.2025.117780.

Gao et al. developed a neural network model that uses six characteristic frequency points from impedance measurements to estimate SOH, without relying on historical impedance data. Validated across multiple datasets, the high-ohmic coin cells used in the study demonstrated promising results.